Thermographic Crack Detection in Hot Steel Surfaces

Philipp MYRACH [1], Benjamin POLOMSKI [1], Elisabeth LE CLAIRE [1],
Sreedhar UNNIKRISHNAKURUP [1], Nitin VENGARA [2],
Krishnan BALASUBRAMANIAM [2], Mathias ZIEGLER [1]
[1] BAM Bundesanstalt für Materialforschung und -prüfung, Berlin, Germany
[2] Indian Institute of Technology Madras, Chennai, India

Contact e-mail: philipp.myrach@bam.de

Abstract. The detection and characterization of surface cracks in steel specimens prior to damage is a technologically and economically highly significant task and is of utmost importance when it comes to safety-relevant structures. In steel production where steel billets at high temperatures have to be inspected while moving a number of well-established NDT methods cannot be applied. Laser thermography however is a promising candidate to serve as a fast, non-contact and remote tool in this case. We present a study that shows that the crack detection capabilities of laser thermography can be extended also to specimens at high temperature. A combination of inductive and laser heating allows to systematically study the contrast formation as well as the optimization of the important measurement parameters. The experiments are accompanied by FEM simulations that provide a better insight of the physical correlations and support the experimental developments. The aim of these studies is to develop a system with high inspection speed and detection performance to be in-line operated under the hostile environment of steel production lines.

Introduction

A constant major task for non-destructive testing is the detection and characterization of surface cracks. Thus a large number of different methods are available today, e.g. eddy current, ultrasound, dye penetration (DPI), magnetic particle (MPI) or computer tomography, for instance. This variety of techniques is due to their specific advantages and restrictions that favour / limit their application to specific conditions. It can even prohibit its applicability as it is the case for the detection of cracks in steel production, where moving steel billet at high temperatures don't allow measurements in contact with the specimen and furthermore very hostile production conditions are present.

Laser-thermography however, as a fast, non-contact and remote technique is believed to be well suited to serve as a NDT method for the detection of surface cracks even at the harsh condition in steel production.

First introduced by Kubiak [1] in 1968, the technique was developed for decades [2, 3] and accompanied by major progress in infrared (IR) detector and laser technology became a powerful tool today [4, 5, 6, 7]. Laser-thermography has already been proven to be well-suited to detect surface cracks in steel [4, 8] and can also compete with other NDT methods [9].

License: http://creativecommons.org/licenses/by/3.0/

More info about this article: http://ndt.net/?id=19573

In this study it is shown that the scope of application can also be extended to the identification of cracks in hot steel (<700°C) by still maintaining the advantages of the technique. The experimental study is accompanied by FEM simulations that will allow for a systematic investigation of the important parameters and further optimization of the measurement and data processing.

Principle and Experimental Parameters

1.1 Principle

To detect surface cracks a focused laser beam is used to locally heat the sample surface, which results in a heat diffusion of spherical rather than planar fashion as it is the case for flash thermography for instance, where the heating is applied homogenously on a large surface area. In case of local heating however, the heat flow is not only oriented perpendicular to the surface, but also parallel and thus surface cracks with a perpendicular orientation also alter the heat diffusion. The heat blocked at the crack edges leads to a characteristic temperature contrast on the surface. Recording and analysing the surface temperature with an IR-camera allows for the identification of surface cracks.
Besides the crack acting as a thermal resistance for the heat flow, also it is a local increase of the absorption, since the laser radiation is reflected multiple times inside the crack, where every time energy is absorbed and thus heating is more efficient within the crack. Furthermore the crack acts as a good emitter for IR-radiation due to its increased surface area compared to flat surface. Both effects lead to a higher thermal radiation recorded by the IR-camera at the place of a crack.

1.2 Setup and Experimental Parameters

In this study a diode laser emitting at 940 nm with a maximal power of 510 W was used as the local heat source. In order to allow high testing speeds additional optics were used to create a line (30 mm x 0.6 mm) rather than a laser spot. To perform experiments at different initial temperatures induction heating (5 kW, 160-400 kHz) was applied to the sample. By controlling the heating power of the induction source the sample could be heated to a maximum temperature of 700 °C. After the sample reached its final temperature at the heating stage (see Fig. 1.) the induction coil was lifted automatically and the sample moved on a linear stage through the field of view of the IR-camera and the static laser line. This procedure was automatized to minimize cooling of the sample after stopping the induction heating and to simulate realistic production conditions, where testing will be done at moving steel billets that pass the laser-thermography testing stage.

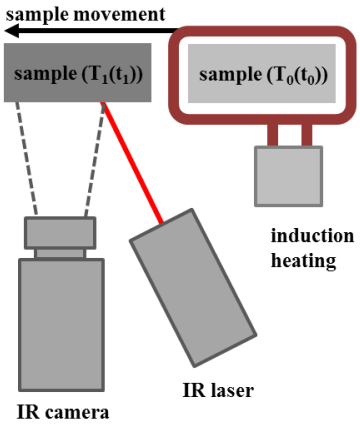

Fig. 1. Schematic representation of the setup. After the sample is heated by the induction heating it moves on a linear stage through the field of view of the IR-camera. At the same time the laser locally heats the sample surface.

The experiments were performed at different initial temperatures of the sample, starting at room temperature (RT) and then subsequently increasing in steps of 100 °C up to a maximum temperature of 700 °C. After pre-heating the sample moved with a speed of 50 mm / s simultaneously heated by the laser line with powers ranging from 50 W to 500 W. The whole passing of the sample is recorded by the IR-camera with a framerate of 200 Hz.

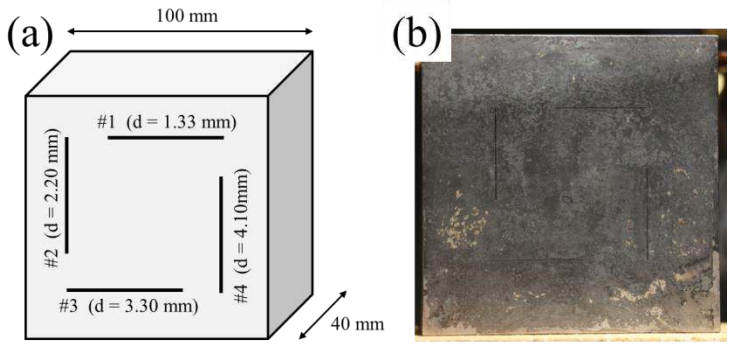

Fig. 2. (a) Scheme of the specimen with the notch position and the respective depth indicated. All notches are 30 mm in length and 0.2 mm in width. (b) Photograph of the specimen made of ST37 steel.

The investigated sample was a block made of ST37 steel, (100 x 100 x 40) mm³ in size containing notches of different dimensions as depicted in Fig. 2. The experiments presented in this paper focus on the notch with 1.33 mm depth (notch #1).

1.3 Data Processing

After the measurement the thermal sequence is rearranged such that a complete image of the sample is generated from the information of one pixel line parallel to the orientation of the laser line. For this reconstruction, if the sample is moving from right to left, a vertical line of pixels at the position of the laser is taken for every time step t (i.e. frame) and rearranged starting left with the line at $t = 0$ and placing the lines with $t > 0$ subsequently on to the right. Since the sample is moving this leads to a complete image of the sample reconstructed of the information at the laser line. By performing this procedure also for lines of pixels on the left side of the laser line, images are generated that show the sample while cooling down after the laser heating.

2. Results

Fig. 3 shows an image reconstructed at the laser line, at t = 0 s, as well as an image reconstructed of a line 20 pixels left of the laser line, corresponding to 0.1 s after the laser heating. The initial temperature of the sample was 500 °C and the applied laser power was 100 W (~550 W / cm²).

It can be observed, that an identification of cracks directly at the time of laser heating is hardly possible. This is due to the strong inhomogeneties of the emissivity on the surface caused by discolorations and the formation of scale while pre-heating. These inhomogeneties dominate the contrast. However, shortly after the sample cools down, the notches form a recognizable contrast (Fig. 3 bottom). These contrast formation was found in all experiments independent of the initial temperature.

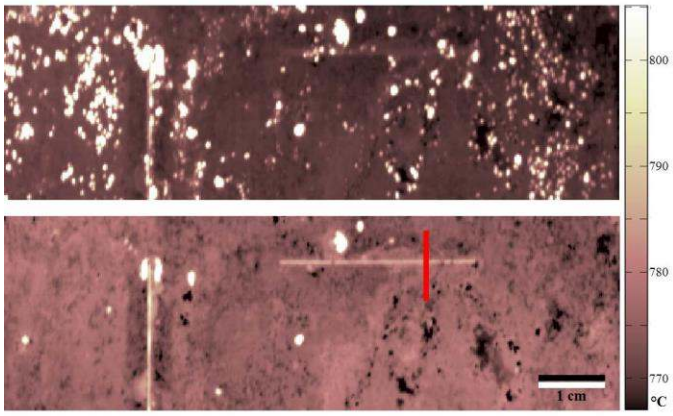

Fig. 3. (Top) Reconstructed image at t = 0 s (@ laser line) for an initial temperature of the sample of 500 °C and a laser power of 100 W, showing notch #1 and #2 (see Fig. 2). (Bottom) Reconstructed image 0.1 s after the laser heating. The red line indicates the position for the temporal analysis performed in Fig. 4.

Fig. 4(a) shows the temporal evolution of a line scan taken perpendicular to the notch indicated in Fig. 3, highlighting the observation that the optimal contrast isn't found at the time of laser illumination, but shortly after it. Furthermore the crack contrast only slowly fades out, purposing that in this case the contrast is mainly governed by the increased absorption and emissivity of the crack. Contrast formation by a heat flow blocked at an interface usually occurs on smaller time scales.

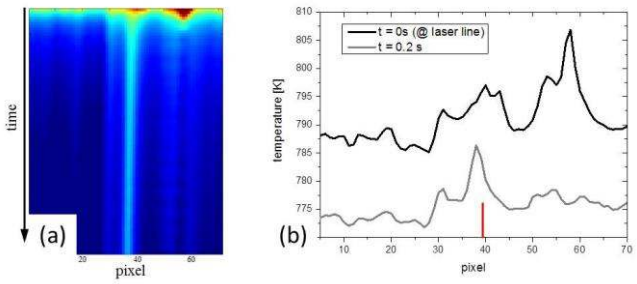

Fig. 4. (a) Line scan for the notch indicated in Fig 3 (notch #1) versus time. The contrast at t = 0s is dominated by the presence of inhomogeneties of emissivity (scale) which can also be seen in (b). After laser heating the sample cools down and the crack contrast start to emerge.

Performing these experiments for different initial temperatures shows that a reasonable crack contrasts can be produced also for temperatures up to 700°C. Fig. 5 shows line scans for each initial temperature with the same scaling. The laser power in all experiments was set to 500 W in order to compare the resulting contrasts. What can be seen is that the crack

contrast is decreasing witch with increasing initial temperature. This implies that the temperature rise induced by the local heating reduces and thus the laser power has to be increased to lead to the same contrast. However, this experiments show that the detection of surface cracks by laser thermography is possible even at elevated temperatures.

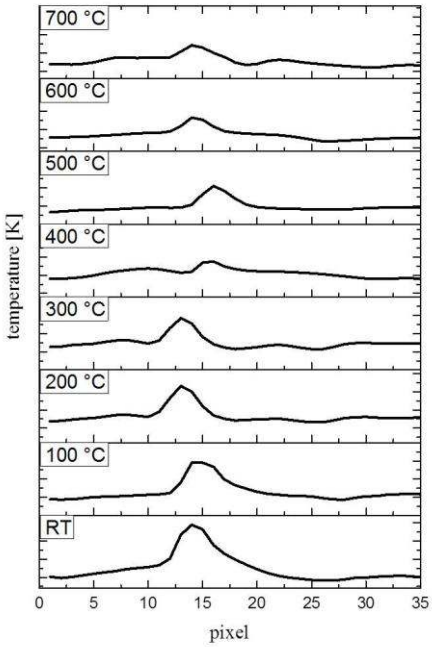

Fig. 5 Line scans for the line indicated in Fig 3. for different initial temperatures of the sample. The laser power was set to 500 W for all measurements. All line scans are plotted with the same scaling.

3. Modeling and simulation

The experimental investigations are accompanied by simulations that will provide a better understanding of the actual contrast mechanism and furthermore allow an optimization of the testing parameters. The simulations using COMSOL Multiphysics v 5.2 focused on a three-dimensional model of the sample described above and a point like local heat source, whereas the initial temperature of the steel block was set to room temperature.

3.1. General and Simulation Parameters

A laser beam illuminating the sample surface generates a temperature gradient, due to which an energy transfer will occur from the high-temperature to the low-temperature region. The heat transfer rate due to conduction per unit area is proportional to the normal temperature gradient:

$$\frac{q}{A} = -k\frac{\partial T}{\partial n}$$

Where q is the heat transfer rate, $\frac{\partial T}{\partial n}$ is the temperature gradient in the direction of the heat flow, and the constant k is the thermal conductivity of the material (W / m·K). The minus sign is inserted to indicate that heat flows from a higher to a lower temperature value. Considering the energy balance in three dimensions the heat conduction equation in 3D in a concise form can be written as:

$$\rho C_p \mathrm{u} \cdot \nabla T + \nabla \cdot (k\nabla T) + \rho C_p \frac{\partial T}{\partial t} = \dot{Q} + Q_{ted}$$

Where $\dot{Q}$ is the heat generation, ρ is the density of the material, and C_p is the specific heat of the material. The initial temperature is room temperature (T_0 = 298 K) for all domains. Table 1 gives the thermal properties of the ST37 steel.

Material property	ST37
Thermal conductivity k ($Wm^{-1}K^{-1}$)	42.7
Specific heat capacity c ($J\ kg^{-1}K^{-1}$)	477
Density ρ (kgm^{-3})	7880

Table. 1. Material parameters for ST37 as used for the simulation.

A surface laser heat source assumes that the beam energy is absorbed over a very small distance into the material (absorption length) compared to the size of the object heated. The finite element mesh only needs to be fine to resolve the temperature fields and the laser spot size. The laser source itself is not explicitly modeled, and it is assumed that the fraction of laser radiation reflected from the surface is not reflected back.

The deposited beam power option is used to model the CW laser beam and a Gaussian laser beam profile is defined as the heat source, written as

$$f(0,e) = \frac{1}{2\pi\sigma^2}\exp\left(-\frac{d^2}{2\sigma^2}\right)$$

with $d = \frac{||e\times(x-O)||}{||e||}$, σ = standard deviation

Typical mesh for FEM simulations is optimized based on two parameters, width of the crack and the laser spot diameter. The free triangular mesh size near the crack is adjusted to 5 times smaller than the width of the crack. Fig. 6 shows the geometry of the sample and the corresponding meshed geometry.

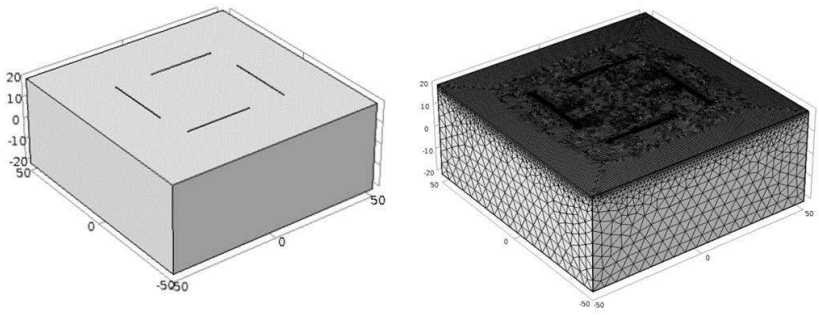

Fig. 6 3D-geometry of the ST37 sample and corresponding mesh used for the simulation.

3.2. Experimental Validation

A set of experiment was acquired to be compared to the simulation results. Instead of a laser line a laser spot scanned the sample surface with different scanning speed. The laser power was set to 20 W. Due to the presence of cracks heat blockage will increase at the left side of the crack according to scanning direction.

We developed a tracking algorithm in order to measure the temperature of a point immediate after the laser passage, i.e. to measure the cooling cycle. We applied the same algorithm which we developed on both experimental and modelling data. From the graph we can clearly identify the presence of crack by the variation in the heat distribution, i.e. there is a temperature rise due to the heat blockage. To validate the simulation data we noted the temperature rise due to the presence of a 0.2 mm opening crack with 3.3 mm across the laser line. Fig. 7 (a) shows the graph plotted by variation of temperature in modelling data whereas Fig. 7 (b) is the same graph plotted using experimental data.

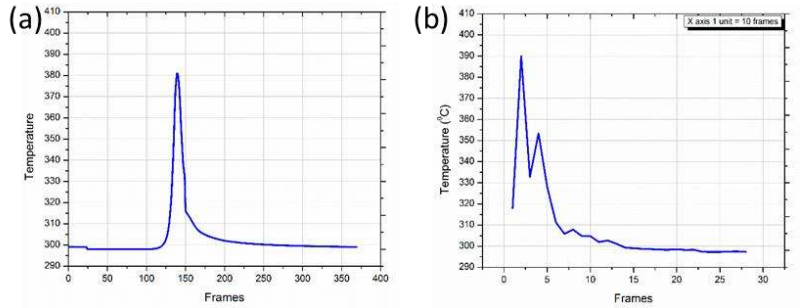

Fig. 7 (a) Temperature versus frames (time) for a point moving with the laser. The temperature rise indicates the presence of a crack. (b) Temperature versus frames for the corresponding experiment.

Both figures show the temperature profile of a point which is following the laser spot at a distance, moving with the same speed. Due to the presence of the crack there is an increased temperature near the crack due to the variation in the thermal heat flow. In both cases the metal surface is cooling very fast to room temperature if there is no disturbance of thermal heat flow. The comparison of simulation and experimental data still shows some variation in the temperature rise and difference in the shape that demand further improvements on the model regarding the laser beam - crack interaction.

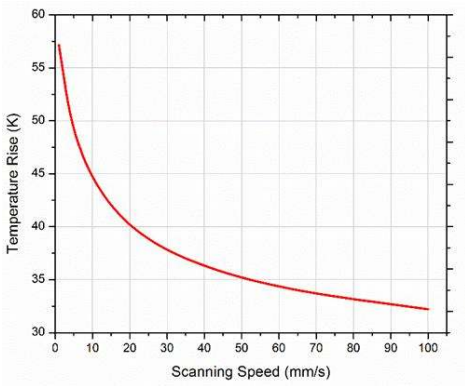

Fig. 8 Simulated temperature rise associated with the presence of a surface crack versus the scanning speed. As the scanning speed (movement of the billets) increases the temperature rise decreases.

However, the vicinity of crack can be detected by the temperature increase due to the thermal blockage. By determining the maximum peak height of the temperature one can compare the temperature rise induced by a crack depending on different measurement parameters. This was done for the scanning speed and is shown in Fig, 9. As scanning speed increases, temperature rise due to the presence of a crack will drastically decrease, meaning that experiments should be performed with the steel billets moving at small speeds.

Of course, the requirements of the production set strict limitations to the moving speed. However, simulations allow to investigate the influence of other measurement parameters,

as the laser power for instance, on the testing results. This will allow a systematic study to find the optimal testing parameters.

4. Conclusion

The presented results show that the good crack detection capabilities of laser thermography can be maintained even for test specimens at high temperature. The setup used within this study also shows that data processing can be adapted in a way that future applications for an online testing and monitoring becomes possible. Since the experimental investigations are assisted by FEM simulations the potential of the method can be efficiently examined and allows developing laser thermography to a powerful and reliable NDT technique.

References

[1] E. J. Kubiak, *"Infrared detection of fatigue cracks and other near-surface defects"*, Applied Optics, **7**(9), 1743(1968)
[2] J.-C. Krapez, L. Legrandjacques, F. Lepoutre and D. L. Balageas, *"Optimization of the photothermal* camera for *crack detection"*, QIRT 1998-048, (1998)
[3] C. Gruss, D. Balageas, *"Theoretical and experimental applications of the flying spot camera"*, Proc. QIRT 92 (Seminar Eurotherm No. 27), 19-24(1992)
[4] J. Schlichting, M. Ziegler, C. Maierhofer, M. Kreutzbruck, *"Efficient data evaluation for thermographic crack detection"*, QIRT Journal, Short Communications 8(1), 119(2011).
[5] P. Joubert, S. Hermosilla-Lara, D. Placko, F. Lepoutre, M. Piroiu, *"Enhancement of open*-crack detection in flying-spot photothermal non-*destructive testing using physical effect identification"*, QIRT Journal Vol. **3/1**, pp 53-70(2006).
[6] S. E. Burrows, A. Rashed, D. P. Almond, S. Dixon, *"Combined laser spot imagi*ng thermography and ultrasonic measurements for crack detection*"*, NDT &E Intern. (Special Issue: Thermographic NDT) **22** (2-3)(2007).
[7]T. Li, D. P. Almond, D. Andrew, S. Rees, B. Weekes, *"Crack imaging by scanning pulsed laser spot thermography"*, NDT&E Intern. **44**, 216(2011)
[8] P. Myrach, M. Ziegler, C. Maierhofer, M. Kreutzbruck, *„*Influence of the acquisition parameters on the performance of laser-thermography for crack detection in metallic component*"*, Proceedings 40th Annual review of progress in quantitative nondestructive evaluation, **1581,** 1624-1630 (2014)
[9] R. Casperson, R. Heideklang, P. Myrach, Y. Onel, M. Pelkner, R. Pohl, R. Stegemann, M. Ziegler, M. Kreutzbruck, *"*Vergleich konventioneller und neuer Oberflächenprüfverfahren für ferromagnetische Werkstoffe*"*, Tagungsband – DACH-Jahrestagung 2015, Salzburg, Austria, DGZfP **BB 152**, (2015)